IET Renewable Power Generation

Special Issue Call for Papers

Be Seen. Be Cited.
Submit your work to a new IET special issue

Connect with researchers and experts in your field and share knowledge.

Be part of the latest research trends, faster.

Read more

The Institution of Engineering and Technology

IET Renewable Power Generation

Research Article

IET Journals
The Institution of Engineering and Technology

Research on power sharing strategy of hybrid energy storage system in photovoltaic power station based on multi-objective optimisation

ISSN 1752-1416
Received on 26th April 2015
Revised on 21st October 2015
Accepted on 4th January 2016
doi: 10.1049/iet-rpg.2015.0199
www.ietdl.org

Wei Jiang ✉, *Lei Zhang, Hui Zhao, Huichun Huang, Renjie Hu*

Jiangsu Provincial Key Laboratory of Smart Grid Technology and Equipment, School of Electrical Engineering, Southeast University, Nanjing 210096, People's Republic of China
✉ *E-mail: jiangwei@seu.edu.cn*

Abstract: Battery/supercapacitor (SC) hybrid energy storage system (HESS) is an effective way to suppress the power fluctuation of photovoltaic (PV) power generation system during radiation change. This study focuses on the power sharing between different energy storage components with two optimisation objectives: energy loss and state of charge of SC. First, the topology of HESS and its connection with PV system are analysed. Second, the control targets of the HESS have been organised as optimisation objectives. A linear weighted summation algorithm based on variable weights is proposed to solve the multi-objective optimisation problem to obtain current reference of SC and battery. Third, the energy management system of the HESS is designed based on proposed algorithms. Simulation and experiment results verified the proposed algorithms and control strategy.

1 Introduction

The distributed generation has been considered as a replacement of fossil fuels to solve urgent environmental problems around the world. The photovoltaic (PV) generation system is widely applied to fulfil the increasing energy demand. The output power of PV generation system fluctuates with such changing climate factors as solar radiation and temperature. It is necessary to install the energy storage devices in a PV generation system to guarantee its stability and power quality in different operating modes [1]. Energy storage devices also mitigate the voltage fluctuation problem under high PV penetration [2, 3]. The consumers would pay less on their electricity bills with the application of PV generation system and controllable storage devices which realise peak shaving on individual power demand profile [4, 5]. We need to strike a balance between power-density and energy-density when deciding which energy storage technology to choose. The hybrid energy storage system (HESS) is an energy storage system that could, by combining an energy-dense source with a power-dense one, store a high amount of energy and supply high peak power when necessary. In this paper, the energy sources of interest are battery and supercapacitor (SC). Compared with battery-only energy storage system, battery/SC HESS has better performance. In [6], the simulation results reveal that the discharge rate and the cumulative ampere-hour (Ah) throughput of battery could be reduced by introducing SC into the battery energy storage system, which could extend the lifetime of the battery. When SC and with lithium-ion battery are assembled together, the overall peak power capacity could rise several times, power loss could be significantly reduced and system volume and weight could be minimally impacted [7]. The battery/SC HESS has been reported in several application fields. In electric vehicle application, the battery/SC HESS is applied to improve driving-range of electric vehicle up to 46% [8–10]. In renewable power generation application, the battery/SC HESS performs well in power quality control [11, 12]. In railway traction application, the battery/SC HESS can reduce the mass and volume of the energy storage system installed on the vehicle [13].

When the battery/SC HESS is applied to PV generation system, the power fluctuation can be suppressed and the ac bus voltage can be stabilised. Thus, the steady and economical operation of PV station can be guaranteed. The HESS can meet two types of demands needed by PV station: the high energy but low-power demand and high power but low-energy demand. Battery can provide long-term stable power but suffers from high charge/discharge rate, so SC could serve as the short-term energy storage component in HESS and relieve battery of dynamic stress. Therefore, the system topology which interfaces SC and battery plays a pivotal role in properly taking advantage of the characteristics of these two energy storage components. Passive HESS has a simple structure but the power flow between the energy sources is uncontrollable, while active HESS with bi-directional dc/dc converters can overcome aforementioned problems and precisely control the power sharing between battery and SC. The possible topologies of active HESS are discussed in [14, 15]. The configuration of the battery and SC connected through their respective dc/dc converters shows better performance because of the decoupled controllability and fault tolerant [16–18], as shown in Fig. 1. In addition, the dc/dc converter connected to SC can boost its terminal voltage to the rated value of common dc bus.

To prolong the lifetime of HESS and adapt it to peak power consumption, a good battery/SC HESS should: (i) reduce the charge/discharge rate and frequency of the battery; (ii) minimise the energy loss of the overall system; (iii) reserve the state of charge (SOC) of SC for peak power demands. The design of energy management system, which controls the power flow coming from battery and SC, is crucial to achieve aforementioned goals. The simplest method to reduce the charge/discharge frequency of the battery is to use a low-pass filter to distinguish between the low-frequency and high-frequency parts of the demanded power. In [19], the moving average filter is utilised to provide the reference of the power delivery command for SC. However, the disadvantage of the low-pass filter is that it could not satisfy all the control goals at the same time, so some intelligent control strategies based on the optimisation theory are adopted. In [20], probability-weighted Markov process is used to predict the future load demands. Real-time decisions on the power sharing between battery and SC are made based on the predictions and probabilities of state trajectories along with associated system losses, and dc/dc converters are controlled by them. A power sharing algorithm which adjusts the boundary parameters based on the multiplicative-increase–additive-decrease principle is introduced in [21]. The proposed algorithm can guarantee a feasible optimal solution within a few iterations. In [22], the

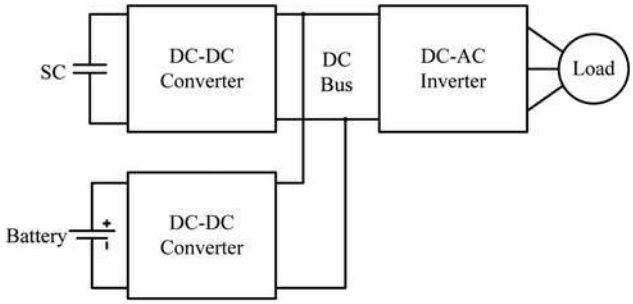

Fig. 1 *Topology of the active HESS with respective dc/dc converters*

real-time decision tree is used to achieve two energy management goals: minimisation of energy loss and maximisation of the power reserve in SC. The Pareto-front for the short-range load profile sets is generated off-line, so the real-time performance of the algorithm is limited.

The main idea of this paper is to propose a multi-objective optimisation algorithm, which comprehensively takes system loss, SOC reservation of SC and power limits into consideration, for the battery/SC HESS energy management system that could be applied to power fluctuation suppressing in PV generation system. Simulation and experiments are conducted to verify the performance of the proposed power sharing algorithm by comparing it with other methods and discussing the effect of optimisation factor.

2 PV power station with HESS

According to the technical regulations of power grid corp., the PV power stations should execute the control instructions from power dispatching department to guarantee the active power and its rate of change. The active power change rate criterion of grid-connected PV station from China State Grid [23] is shown in Table 1.

Owing to the climate factors, the active power fluctuation of PV station could violate the technical regulations in Table 1. Under these conditions, the HESS serves as an energy buffer that stores energy at active power peak and relieves energy at active power valley to suppress the active power fluctuation of PV station. Inside the HESS, battery responds to low-frequency power demand and SC responds to high-frequency power demand with their respective bi-directional dc/dc converters. The structure of grid-connected PV station with HESS is shown in Fig. 2.

As shown in Fig. 2, an ac–dc hybrid structure is applied, providing a reliable and flexible approach to integrating distributed energy resources and energy storage components into utility grids. This hybrid structure enables dc/dc converters to regulate the dc voltages of battery and SC, and thus meet the dc side voltage requirement of dc–ac invertors. Meanwhile, the power sharing control could be easily realised with dc bus, since the output power of energy storage components could be adjusted by controlling their respective current reference. In the proposed system, PV Array1–PV Array$N$ are connected to the dc bus via dc–dc converter 1.1–1.N. The output power of PV arrays p_{v1}–p_{vN} are regulated at maximum power point by maximum power point

Table 1 Maximum active power change of PV station

Station type	Voltage class	Maximum active power change in 10 min, MW	Maximum active power change in 1 min, MW
small	0.4 kV	installed capacity	0.2
medium	10–35 kV	installed capacity	installed capacity/5
large	66 kV or above	installed capacity/3	installed capacity/10

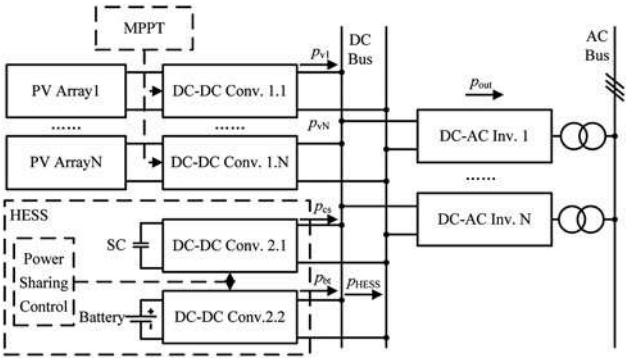

Fig. 2 *Structure of grid-connected PV power station with HESS*

track controller. The overall power of PV arrays is $p_v = \sum_{i=1}^{N} p_{vi}$. The power extracted from SC (p_{cs}) and battery (p_{bt}) is regulated by controlling the output current of bi-directional dc–dc converter 2.1 and dc–dc converter 2.2. To achieve high boost ratio and efficiency, isolated bi-directional could be applied [24]. The current references of these two converters are provided by the energy management system which realises the proposed power sharing algorithm. The overall power of HESS is $p_{HESS} = p_{cs} + p_{bt}$ and that of PV station is $p_{out} = p_v + p_{HESS}$. p_{HESS} suppresses the power fluctuation of PV system to conform with the maximum active power change regulations.

3 Power sharing algorithm with multi-objective optimisation

3.1 Optimisation objectives

To optimise the distribution of power between the two energy storage components, we have to set targets for the power sharing of the energy management system of the HESS. In battery/SC HESS, the battery has relatively smaller power capacity and shorter charge/discharge cycle lifetime. Therefore SC, if reserves sufficient energy capacity, should contribute to the higher frequent part of p_{HESS}. Meanwhile, considering the cost and volume of HESS, the energy capacity of SC is usually limited. Thus the SOC of SC, which is defined as SOC_{sc}, could easily reach its upper/lower limits denoted as $SOC_{sc.max}$ and $SOC_{sc.min}$. If the SOC_{sc} exceeds over $SOC_{sc.max}$, the sudden positive power demand ($p_{HESS} > 0$) cannot be met. If the SOC_{sc} drops below $SOC_{sc.min}$, the sudden negative power demand ($p_{HESS} < 0$) cannot be met. If the higher frequent part of p_{HESS} is obtained through conventional low-pass filter without considering the capacity limit, SC may not be able to completely respond to the power demand. Under this circumstance, battery is forced to charge/discharge at higher frequency, which could shorten its lifetime. Therefore, the energy management system should properly control the power flow of SC and of battery to maintain reasonable SOC of SC.

On the other side, given the difference in internal resistance between SC and battery, the strategy adopted for the power sharing would affect the overall efficiency and operation time of the system. Therefore, setting up an energy loss model for the system is an indispensable part of creating a strategy for power sharing. To comprehensively optimise the SOC_{sc} and to reduce the energy loss of the system, we take the following two objectives into account when we design the power management system:

i. To minimise the overall system energy loss $e_{HESS.loss}$ of HESS to guarantee its efficiency.
ii. To keep SOC_{sc} within the optimal range to reserve energy capacity of SC for future demand.

Mathematically speaking, this problem is called a multi-objective optimisation problem (MOP). An MOP could be expressed as

IET Renew. Power Gener., 2016, Vol. 10, Iss. 5, pp. 575–583

$$\min_{x\in S\subseteq R^n} \boldsymbol{F}(x) \tag{1}$$

In (1), the feasible region is denoted as S. The vector of objective functions is denoted as $\boldsymbol{F}$: $R^n \to R^k$, $\boldsymbol{F}(x) = (f_1(x), \ldots, f_k(x))^{\mathrm{T}}$. Moreover, x is the optimisation variable.

To achieve the objectives of optimisation, we need to express the MOP with the mathematic models of $\mathrm{SOC_{sc}}$ and of the energy loss of the system. Since the energy management system has to work in real-time digital controller, the MOP should be solved fast and effectively, which we will introduce in the following section.

3.2 Description and resolution of the MOP

Since SC and battery are parallel-connected to dc bus through bi-directional dc/dc converters, the terminal voltages of the two dc/dc converters are identical. Meanwhile, p_{HESS} only consists of the power extracted from battery (p_{bt}) and the power extracted from SC (p_{sc}). Consequently, only one current variable is needed to control the power sharing ratio between battery and SC. In this paper, the control variable is battery current i_{bt}. The SC current can be derived as

$$i_{\mathrm{sc}} = \frac{p_{\mathrm{HESS}}}{v_{\mathrm{bus}}} - i_{\mathrm{bt}} \tag{2}$$

where v_{bus} is the voltage of dc bus.

As discussed above, before we try to distribute the power optimally between the energy storage components, the MOP should be expressed mathematically. The first step is to construct the energy loss and the $\mathrm{SOC_{sc}}$ models.

The overall power loss of HESS is defined as p_{loss}. p_{loss} consists of four parts: SC internal loss $p_{\mathrm{sc.loss}}$, battery internal loss $p_{\mathrm{bt.loss}}$, dc/dc converter loss $p_{\mathrm{conv2.1.loss}}$ and $p_{\mathrm{conv2.2.loss}}$. Therefore, p_{loss} could be expressed as

$$p_{\mathrm{loss}} = p_{\mathrm{sc.loss}} + p_{\mathrm{bt.loss}} + p_{\mathrm{conv2.1.loss}} + p_{\mathrm{conv2.2.loss}} \tag{3}$$

The four parts in (3) can be calculated with: $p_{\mathrm{sc.loss}} = (i_{\mathrm{sc}}/(1-d_{2.1}))^2 \cdot R_{\mathrm{sc}}$, R_{sc} is the equivalent internal resistance of SC; $p_{\mathrm{bt.loss}} = (i_{\mathrm{bt}}/(1-d_{2.2}))^2 \cdot R_{\mathrm{bt}}$, R_{sc} is the equivalent internal resistance of battery (see equation at the bottom of the page)

where $d_{2.1} = 1 - (v_{\mathrm{sc}}^{cc}/v_{\mathrm{bus}})$ is the duty ratio of dc/dc Conv. 2.1; $d_{2.2} = 1 - (v_{\mathrm{bt}}^{cc}/v_{\mathrm{bus}})$ is the duty ratio of dc/dc Conv. 2.2; v_{sc}^{cc} is the open-circuit voltage of SC; v_{bt}^{cc} is the open-circuit voltage of battery; t_{r} and t_{f} are rising and falling time of Q_1 and Q_2; R_{L} is the equivalent resistance of inductor L; R_{Q1} and R_{Q2} are on-resistances of Q_1 and Q_2; and f_{s} is the switching frequency of Q_1 and Q_2. There is $i_{\mathrm{sc}} = (\Delta p v_{\mathrm{bus}}) - i_{\mathrm{bt}}$.

The $\mathrm{SOC_{sc}}$ depends on its initial value and the charge/discharge power (see (4))

where $\mathrm{SOC_{sc}}(t)$ is the $\mathrm{SOC_{sc}}$ at the end of t; ρ is the self-discharge rate of SC; η is the charge/discharge efficiency of SC; $V_{\mathrm{sc.max}}$ is the maximum terminal voltage of SC; $V_{\mathrm{sc.min}}$ is the minimum terminal voltage of SC; and C_{sc} is the capacity of SC.

The objective function for system energy loss optimisation P_1 can be expressed as

$$(P_1)\begin{cases} \min & e_{\mathrm{loss}}(i_{\mathrm{bt}}) = \int_0^T p_{\mathrm{loss}}(i_{\mathrm{bt}})\,\mathrm{d}t \\ \text{s.t.} & i_{\mathrm{HESS}} - i_{\mathrm{sc.max}} \le i_{\mathrm{bt}} \le i_{\mathrm{bt.max}} \end{cases} \tag{5}$$

P_1 indicates that i_{bt} should be adjusted to minimise the system energy loss e_{loss}, which is the integral of p_{loss}. Meanwhile, the in/out currents of battery and SC should be limited in the rated ranges. The upper limit is the maximum output current of the battery ($i_{\mathrm{bt.max}}$). The lower limit is the difference between the output current of HESS (i_{HESS}) and the maximum output current of SC ($i_{\mathrm{sc.max}}$).

The objective function for $\mathrm{SOC_{sc}}$ optimisation P_2 can be expressed as

$$(P_2)\begin{cases} \min & S(i_{\mathrm{bt}}) = \dfrac{1}{T}\displaystyle\int_0^T \left(\frac{\mathrm{SOC_{sc}}(i_{\mathrm{bt}}) - \mathrm{SOC_{sc}^*}}{\mathrm{SOC_{sc.max}} - \mathrm{SOC_{sc.min}}}\right)^2 \mathrm{d}t \\ \text{s.t.} & i_{\mathrm{HESS}} - i_{\mathrm{sc.max}} \le i_{\mathrm{bt}} \le i_{\mathrm{bt.max}} \end{cases} \tag{6}$$

P_2 indicates that i_{bt} should be adjusted to let $\mathrm{SOC_{sc}}$ approach its reference $\mathrm{SOC_{sc}^*}$, where $\mathrm{SOC_{sc}^*} = \mathrm{SOC_{sc.low}}$ when SC provides positive power, $\mathrm{SOC_{sc}^*} = \mathrm{SOC_{sc.high}}$ when SC provides negative power. The optimal range of $\mathrm{SOC_{sc}}$ ($\mathrm{SOC_{sc.low}}$–$\mathrm{SOC_{sc.high}}$) is determined by such factors as the storage capacity of HESS, the boost ratio of the bi-directional dc/dc converter, the required respond speed etc. In our paper, $\mathrm{SOC_{sc.low}}$ and $\mathrm{SOC_{sc.high}}$ are preset according to engineering experiences.

With two given feasible solutions of i_{bt}, i.e. i_{bt1}, $i_{\mathrm{bt2}} \in R$, the results of objective functions P_1 and P_2 cannot be directly compared. We propose a linear weighted summation algorithm based on variable weights to solve above MOP. First, P_1 is converted to a dimensionless problem P_1' to void the direct comparison between P_1 and P_2

$$(P_1')\begin{cases} \min & U(i_{\mathrm{bt}}) = \dfrac{1}{T}\displaystyle\int_0^T \left(\frac{p_{\mathrm{loss}}(i_{\mathrm{bt}}) - p_{\mathrm{loss.min}}}{p_{\mathrm{loss.max}} - p_{\mathrm{loss.min}}}\right)^2 \mathrm{d}t \\ \text{s.t.} & i_{\mathrm{HESS}} - i_{\mathrm{sc.max}} \le i_{\mathrm{bt}} \le i_{\mathrm{bt.max}} \end{cases} \tag{7}$$

where $p_{\mathrm{loss.max}}$ and $p_{\mathrm{loss.min}}$ are the maximum and minimum values of p_{loss}.

There is a trade-off between the optimisation control of $\mathrm{SOC_{sc}}$ and of the energy loss of the system, controlled by i_{bt} in accordance with the changing situation. Since the internal resistance of SC is far smaller than that of battery, its discharge power loss is also lower. When SC provides positive power and $\mathrm{SOC_{sc}}$ is at high level, smaller i_{bt} could diminish e_{loss} and accelerates the decrease of $\mathrm{SOC_{sc}}$. When $\mathrm{SOC_{sc}}$ approaches its lower $\mathrm{SOC_{sc.low}}$, i_{bt} should be increased to slow down the decrease of $\mathrm{SOC_{sc}}$. However, increased i_{bt} means increased power loss. Thus, we bring in an optimisation factor λ to present this trade-off. The optimisation factor is defined as $\lambda = (\mathrm{SOC_{sc}} - \mathrm{SOC_{sc.min}}/\mathrm{SOC_{sc.max}} - \mathrm{SOC_{sc.min}}) \cdot \lambda_0$, where λ_0 is the initial value of λ. With dimensionless problems P_1 and P_2 and the optimisation factor, a single objective optimisation problem single-object problem (SP) is constructed

$$(\mathrm{SP})\begin{cases} \min & F(i_{\mathrm{bt}}) = \lambda U(i_{\mathrm{bt}}) + (1-\lambda) S(i_{\mathrm{bt}}) \\ \text{s.t.} & i_{\mathrm{HESS}} - i_{\mathrm{sc.max}} \le i_{\mathrm{bt}} \le i_{\mathrm{bt.max}} \end{cases} \tag{8}$$

$$p_{\mathrm{conv2.1.loss}} = v_{\mathrm{bus}} \cdot f_{\mathrm{s}} \cdot \left|\frac{i_{\mathrm{sc}}}{1-d_{2.1}}\right| \cdot (t_{\mathrm{r}} + t_{\mathrm{f}}) + \left(\frac{i_{\mathrm{sc}}}{1-d_{2.1}}\right)^2 \cdot \left(R_{\mathrm{L}} + d_{2.1} \cdot R_{Q1} + \left(1 - d_{2.1} \cdot R_{Q2}\right)\right);$$

$$p_{\mathrm{conv2.2.loss}} = v_{\mathrm{bus}} \cdot f_{\mathrm{s}} \cdot \left|\frac{i_{\mathrm{bt}}}{1-d_{2.2}}\right| \cdot (t_{\mathrm{r}} + t_{\mathrm{f}}) + \left(\frac{i_{\mathrm{bt}}}{1-d_{2.2}}\right)^2 \cdot \left(R_{\mathrm{L}} + d_{2.2} \cdot R_{Q1} + \left(1 - d_{2.2} \cdot R_{Q2}\right)\right);$$

$$\mathrm{SOC_{sc}}(t) = (1-\rho)\mathrm{SOC_{sc}}(t-1) + \frac{-\mathrm{sgn}(p_{\mathrm{HESS}}) \cdot \left|p_{\mathrm{HESS}} - i_{\mathrm{bt}} \cdot v_{\mathrm{bus}}\right| \cdot \Delta T \cdot \eta}{0.5 \cdot C_{\mathrm{sc}} \cdot \left(V_{\mathrm{sc.max}}^2 - V_{\mathrm{sc.min}}^2\right)} \tag{4}$$

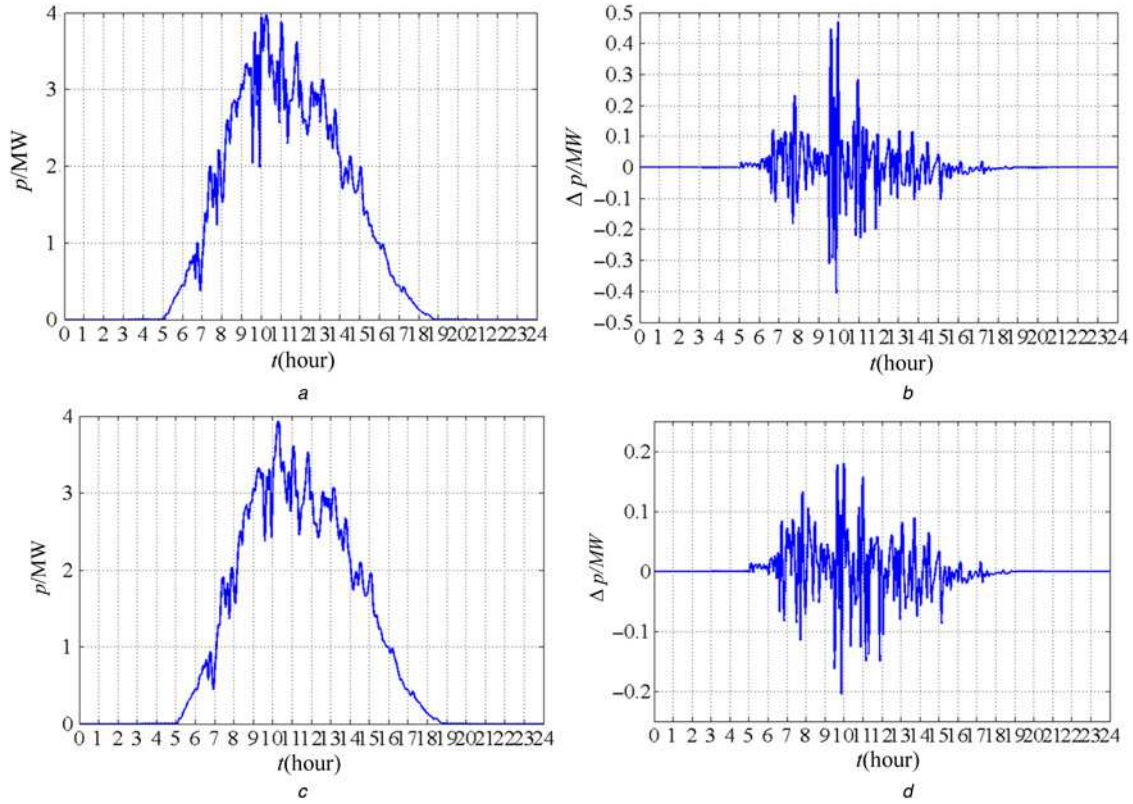

Fig. 3 *Simulation of LPF-VTC*

a Output power of PV station p_v
b Active power change in 1 min of p_v
c Output power reference obtained with LPF-VTC p_{out}
d Active power change in 1 min of p_{out}

By solving SP, the optimal reference current of battery $i_{bt.ref}$ is obtained with varied SOC_{sc}. $i_{bt.ref}$ and derived reference current of SC $i_{sc.ref}$ are output current references of dc–dc Conv. 2.2 and dc–dc Conv. 2.1. Varying with λ_0, the optimisation target could be adjusted between the minimum energy loss and optimised SOC_{sc}. When SOC_{sc} approaches $SOC_{sc.min}$, λ approaches 0. There is $F(i_{bt}) \simeq S(i_{bt})$. The target of SP is to let SOC_{sc} approach its reference SOC^*_{sc} without considering the energy loss. Thus the reserved energy of SC could rise to SOC_{low} very soon. When SOC_{sc} approaches $SOC_{sc.max}$ and the power sharing strategy tends to evenly balance energy loss and optimised SOC_{sc}, we could set $\lambda_0 = 0.5$. There is $\boldsymbol{F}(i_{bt}) = 0.5U(i_{bt}) + 0.5S(i_{bt})$. If the strategy tends to minimise the energy loss, we could set $\lambda_0 = 1$. There is $\boldsymbol{F}(i_{bt}) = U(i_{bt})$. In other conditions, λ_0 could be adjusted between 0 and 1 depending on the preference of the system manager. As space is limited, the optimisation design of λ_0 is beyond the scope of this paper. The effect of λ_0 on optimisation result will be verified in experiment. In practice, an interior point method [25, 26] is used to solve the optimisation problem SP. Since the total processing time of one optimisation period (<1 s) is far shorter than the control command update period (several minutes), the MOP algorithm can be applied in real time in HESS system.

4 Power management of HESS

4.1 Low-pass filtering algorithm with variable time constant

The sum of the power of the two energy storage components has to be equal to p_{HESS}. Thus, the output power p_{out} of the PV station should be determined first, and then the power reference can be calculated based on the equation $p_{HESS} = p_{out} - p_v$. Since the frequency of the power fluctuation of the PV stations is unstable, we cannot simply use a low-pass filter with fixed time constant to obtain p_{out} from p_v. To precisely track the active power change rate criterion, we propose a low-pass filtering algorithm with variable time constant (LPF-VTC). With the proposed algorithm, the output power p_v of the monitored PV array in each optimisation period is processed to obtain p_{out}.

The optimisation period is set to $\Delta T = 1$ min. At $t_k = k\Delta T$, based on discrete LPF formula, there is

$$\tau_k \frac{p_{out.k} - p_{out.k-1}}{\Delta T} + p_{out.k} = p_{v.k} \tag{9}$$

The time constant of digital low-pass filter at t_k is denoted as τ_k. The output power of the PV station at t_k and t_{k-1} are, respectively, denoted as $p_{out.k}$ and $p_{out.k-1}$. The output power of the PV array at t_k is denoted as $p_{v.k}$. According to the 1 and 10 min maximum active power change regulations of PV stations from Table 1, there are

$$p_{out.k} - p_{out.k-1} \le 2 \times 10^5 \tag{10}$$

$$\max\{p_{out.k+i},\ i = 1,\ 2,\ \ldots,\ 10\} - \min\{p_{out.k+i},\ i = 1,\ 2,\ \ldots,\ 10\} \le p_e \tag{11}$$

where the installed capacity of the PV station is denoted as p_e.

From (9), the reference of p_{out} at t_k is

$$p_{out.k} = \alpha_k p_{out.k-1} + (1 - \alpha_k) p_{v.k} \tag{12}$$

where $\alpha_k = \tau_k/(\tau_k + \Delta T)$.

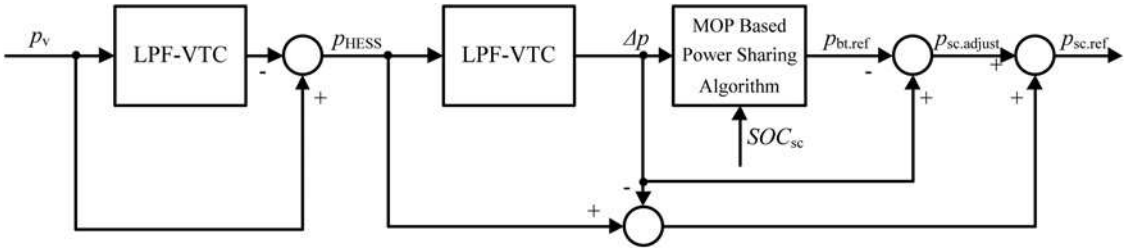

Fig. 4 *Control scheme of HESS power flow for energy management system*

It is assumed that $p_{out.k} \simeq \alpha_{k-1} p_{out.k-1} + (1-\alpha_{k-1}) p_{v.k}$. The time-constant τ_k should follow:

$$\tau_k \geq \max\left(\frac{p_{v.k} - p_{out.k}}{2 \times 10^5}, \frac{p_{v.k} - p_{out.k}}{p_e}\right) \quad (13)$$

On the basis of (13), if the value of τ_k is updated in every optimisation period, $p_{out.k}$ can be calculated with (12) and (13), and then the power reference of HESS at t_k can be obtained based on the equation $p_{HESS.k} = p_{out.k} - p_{v.k}$.

As shown in Fig. 3*a*, the 24 h output power of Xiexin PV station in Xuzhou, China is monitored and depicted as p_v. The amplitude of variation between every two adjacent points of p_v are calculated in MATLAB, as shown in Fig. 3*b*. It is obvious that the maximum amplitude of variation of the active power exceeds 0.2 MW, which violates the regulation for small-scale PV station. To verify the proposed LPF-VTC algorithm, it is programmed in MATLAB as a function *vtcfilter* based on (9)–(13). As shown in Fig. 3*c*, p_{out} is the result of *vtcfilter* with p_v as the input. The amplitude of variation of the active power between every two adjacent points of p_{out} is calculated in MATLAB. It can be seen in Fig. 3*d* that the maximum amplitude of variation has been limited within 0.2 MW. Thus, it is verified that the proposed filter algorithm could be used to obtain the desired output power of the PV station.

4.2 Power flow control

The control scheme of HESS power flow is shown in Fig. 4. As discussed above, the control over the power flow, relying on LPF-VTC algorithm, first obtains the reference of p_{HESS} from p_v. Considering the maximum charge/discharge rate of the battery, the low-frequency part Δp to which battery could respond should be separated from p_{HESS}. The high-frequency part $p_{HESS} - \Delta p$ could only be provided by SC. We use LPF-VTC under the regulation of battery power change rate to obtain Δp. At this time, τ_k is determined by the maximum active power change rate of the battery rather than that of the PV station. In this paper, the maximum current change rate of battery is set to $2i_r$ in 5 s, where i_r is the nominal discharge rate of the battery. Thus, in the filtering period of the second LPF-VTC, there is

$$\tau_k \geq \frac{p_{HESS.k} - \Delta p_k}{2i_r} \quad (14)$$

where $p_{HESS.k}$ is the value of p_{HESS} at t_k and Δp_k is the value of Δp at t_k. With (14), Δp can be obtained. The SC could provide the maximum discharge current, which is up to thousands of amperes, in a period as short as 10 ms. Thus, the difference between p_{HESS} and Δp could be responded by SC.

Since Δp could be provided by both SC and battery, it could be used as the input of the proposed MOP-based power sharing algorithm. With system parameters and monitored voltage/current/SOC_{sc}, the SP in (8) is solved in real time to get optimised output power reference for battery $p_{bt.ref}$. The difference between Δp and $p_{bt.ref}$ is $p_{sc.adjust}$, which represents the lower-frequency part in Δp that is needed to be delivered by SC for SOC_{sc} and energy loss optimisation. Thus, the reference of SC output power is obtained with $p_{sc.ref} = p_{HESS} - \Delta p + p_{sc.adjust}$.

5 Simulation and experiment results

To investigate the performance of the proposed algorithm in power fluctuation suppression, system level model of PV station is built with the structure in Fig. 2 in MATLAB/Simulink. The simulation system parameters are listed in Table 2. Since we accelerated the simulation process to simulate the 24 h operation of HESS in several minutes, the capacities of the battery and the SC are diminished as well. Thus, we could obtain reasonable SOC values from the model. In the system in practice, the energy storage components should have dozens times of capacity to be charged and discharged with large current.

Three different power sharing strategies are simulated and compared with the same model. The simulated strategies are described as follows:

i. *Look-up table (LUT) strategy:* When LUT strategy is used, the power sharing ratio between battery and SC is determined by a preset LUT based on the SOC_{sc}. This strategy is devoted to adjusting the SOC_{sc} to 0.5 for future positive/negative power demands. The LUT used in the simulation is shown in Table 3.
ii. *LPF strategy:* With LPF strategy, a low-pass filter splits the high-/low-frequency parts from the power demand. Battery responds to the low-frequency part and SC responds to the high-frequency part. Saturation blocks are used to prevent output currents of battery/SC

Table 2 Simulation system parameters

Parameters	Value	Units
SC		
rated voltage	50	V
rated capacitance	14	F
equivalent series resistor (ESR)	0.1	Ω
initial SOC	0.5	
Battery		
open circuit voltage	48	V
rated capacity	5	Ah
battery ESR	0.8	Ω
initial SOC	0.95	
PV system		
dc bus voltage	400	V
dc bus input inductance	0.05	mH
dc bus capacitance	1600	μF
maximum active power change in 1 min	200	kW
dc/dc Converter		
switching frequency	20	kHz
inductor	20	μH
inductor ESR	3	mΩ
switch on-resistance	5	mΩ
raising time of switches	32	ns
falling time of switches	20	ns
Proposed MOP algorithm		
$SOC_{sc.min}$	0.25	–
$SOC_{sc.max}$	0.95	–
$SOC_{sc.low}$	0.5	–
$SOC_{sc.high}$	0.8	–
λ_0	0.3	–
optimisation period	1	min

Table 3 LUT strategy power sharing ratio

SOC_{sc}	Power sharing ratio between SC and battery (SC: battery)	
	When $p_{HESS} > 0$	When $p_{HESS} < 0$
0–0.3	0	1
0.3–0.45	0.3	0.7
0.45–0.6	0.6	0.4
0.6–0.75	0.4	0.6
0.75–0.9	0.7	0.3
0.9–1.0	1	0

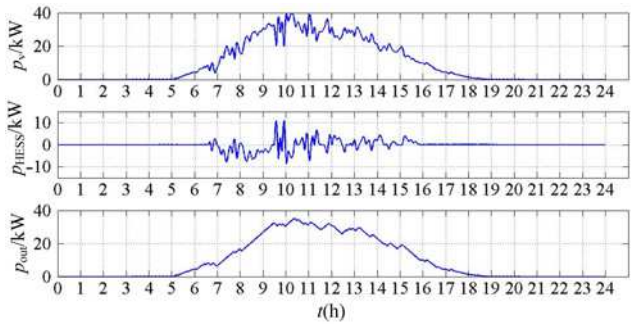

Fig. 5 *Power fluctuation suppressing target of Hongbao PV station 3# main inverter*

from exceeding rated limits. The time constant of the LPF is set to $\tau = 0.6$ s.

iii. *MOP strategy:* With the proposed algorithm, the power sharing ratio is the result of an MOP. Multiple objectives are considered, i. e. energy loss, SOC reservation of SC and output power limits of energy storage components.

The target of the HESS is to suppress the power fluctuation: namely, to restrict the active power change rate of PV station to power grid corp. standard as shown in Table 1. The output power data of PV arrays is obtained from Hongbao PV station 3# main inverter, Zhangjiagang, China. The curves of PV arrays output power p_v, of suppressed power output target p_{out} and of HESS power output demand p_{HESS} are shown in Fig. 5. p_{HESS} and p_{out} are obtained by the proposed LPF-VTC.

The SOC_{sc} waveforms of the three strategies are shown in Fig. 6*a*. The performances are analysed as follows:

i. On the basis of LUT strategy, the preset power sharing ratios help keep the SOC_{sc} around median value (0.5–0.6), so the SC is able to respond to future power demands from both directions.

ii. On the basis of LPF strategy, the SOC_{sc} from 7 o'clock to 10 o'clock is higher than the upper limit of the optimal range, because the negative high-frequency power is the dominant part of p_{HESS} over that period of time. The LPF with fixed time constant raises the power sharing ratio to absorb excessive negative power into SC. Thus the ability of SC to respond to future negative power is diminished.

iii. With the proposed MOP algorithm, the SOC_{sc} keeps at the optimal range (0.5 – 0.8). That is because the MOP automatically adjusts power sharing ratio to track SOC_{sc}^{*} in real time.

The output currents of battery in the three strategies are compared in Fig. 8*b*. Since the power fluctuation frequency factor is considered in LPF and MOP strategies, the battery only provides low-frequency currents. The LUT strategy, though keeps the SOC_{sc} at an optimal range, makes the battery current suffer severe fluctuation. In

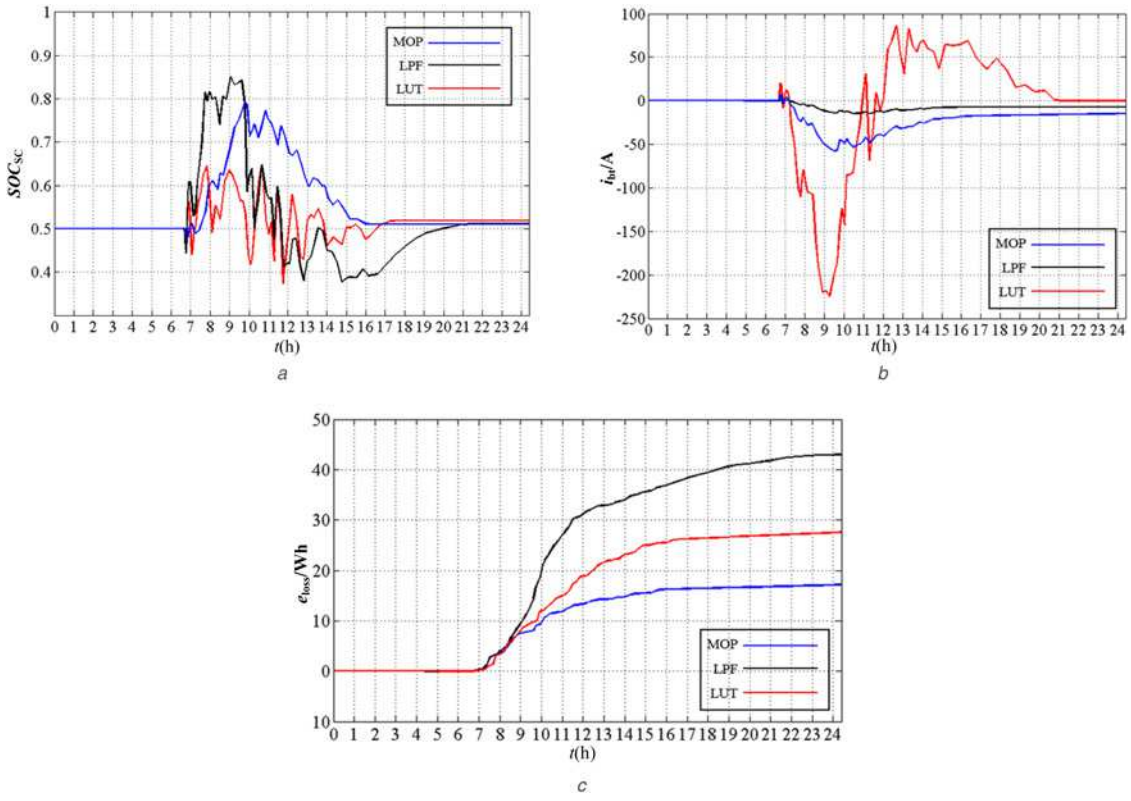

Fig. 6 *Simulation waveforms of three strategies*

a SOCs of SC
b Output current
c Energy loss

IET Renew. Power Gener., 2016, Vol. 10, Iss. 5, pp. 575–583

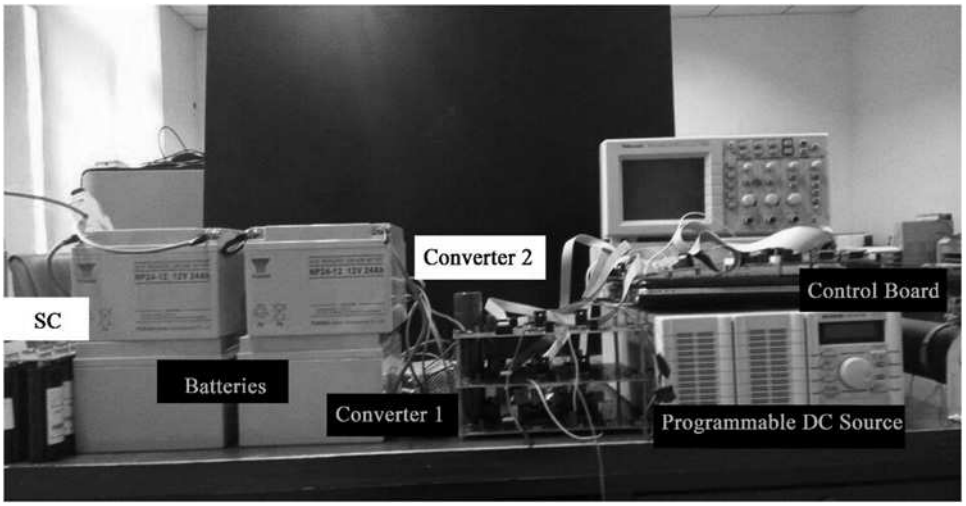

Fig. 7 *Experimental setup*

contrast, the current peak based on MOP algorithm is 58 A (out of the battery) as opposed to 223 A in LUT strategy, showing a significant reduction of 74%. On the basis of LPF strategy, the current could be further reduced if the time constant is large enough but the SOC_{sc} cannot be kept at an ideal range since the SC has to provide proportionately more current.

Fig. 8*c* shows the energy loss curves of the three strategies. Since the minimum energy loss objective is considered in the computation of the reference currents of battery and SC, the energy loss of MOP algorithm is lower than that of others. The simulation result clearly shows that the MOP algorithm could automatically maintain a reasonable SOC_{sc} and minimise the energy loss of the system.

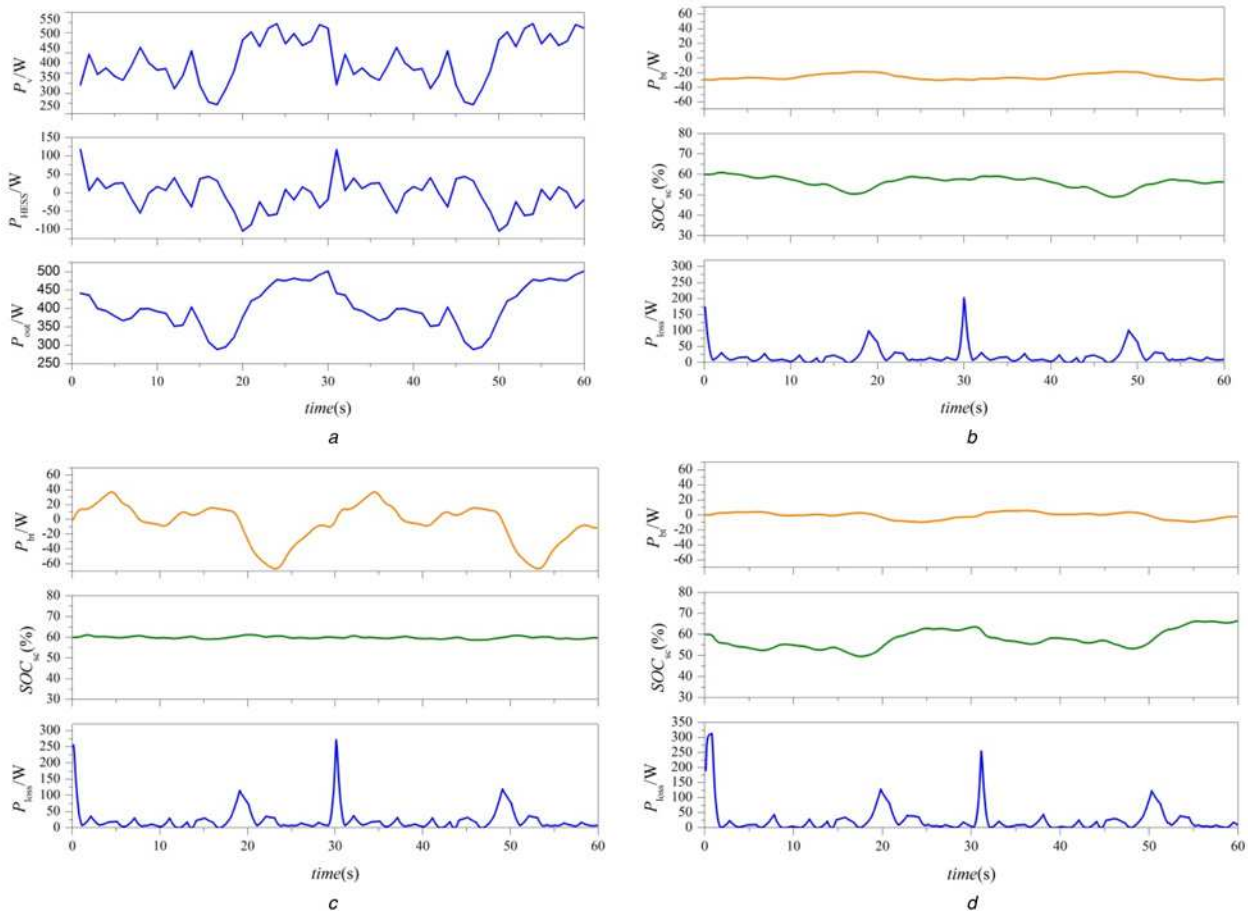

Fig. 8 *Experiment waveforms*

a Compensation target
b MOP strategy with $\lambda_0 = 0.8$
c MOP strategy with $\lambda_0 = 0.3$
d LPF strategy waveforms

Table 4 Experiment parameters

Parameters	Value	Units
rated SC voltage	30	V
rated SC capacitance	3	F
battery voltage	24	V
rated battery capacity	48	Ah
switching frequency	20	kHz
inductance of converter 1	2	mH
inductance of converter 2	5	mH
output capacitance of converter 1	1000	μF
output capacitance of converter 2	1200	μF
dc load	3.5	Ω

As shown in Fig. 7, a low-voltage laboratory prototype, where nominal battery and SC voltages are kept, respectively, at 24 and 30 V, is built. Two bi-directional buck/boost converters are used to interface battery bank and SC module. A control board consisting of TMS320F28335 digital signal processor and XC9500XL high-performance complex programmable logic device (CPLD) is used to monitor energy storage components and control the converters. The SOCs of battery and SC are estimated with Ah integration approach. The algorithms are implemented in personal computer (PC)-based software to calculate the references of i_{bt} every minute. The monitoring data and the current reference are interchanged between control board and PC with TCP/IP protocol via Ethernet connection.

A 1500 W programmable dc source is used to simulate the output power of PV array. Two-and-a-half-hour output power data of 3# main inverter in Hongbao PV station were selected and shrank to <1000 W. To verify the stability of our power sharing algorithm, the data repeats twice in the programmable dc source. The maximum active power change rate also shrank to not exceed 60 W per minute. The simulated output power of PV array (p_v), the power provided by HESS (p_{HESS}) and the suppressed power (p_{out}) are monitored in the experiment as shown in Fig. 8*a*. The dc bus voltage is determined by p_{out} and regulated by dc–dc Conv. 2.1. dc Source and dc–dc Conv. 2.2 both provide current to supply dc load. Table 4 lists all experimental parameters.

In the experiments, we compared the performances of MOP strategy with LPF strategy and verified the influence of λ_0 on optimisation objectives. The initial optimisation factors λ_0 were configured to 0.8 and 0.3, respectively. As shown in Figs. 8*b* and 8*c*, when $\lambda_0 = 0.8$, the solution of MOP tends to minimise system energy loss. As a result, SC compensates most of the high-frequency part of P_{HESS} and the maximum deviation of the SOC_{sc} from its reference value is about 10%. By comparison, when $\lambda_0 = 0.3$, the high-frequency part of the battery output power increases. Consequently, the deviation of SOC_{sc} significantly decreases. However, the overall power loss increases by more than 30% because the energy storage component with larger internal resistance provides more power. The experiment result proves that the objectives of the HESS could be dynamically adjusted by setting λ_0 as we discussed in Section 3.2.

The experiment waveforms of LPF strategy with time constant $\tau = 0.6$ s is shown in Fig. 8*d*. With this configuration, the battery provides low-frequency power which fluctuates around 0. Thus, the deviation of SOC_{sc} from its reference is significant. Meanwhile, the average power loss is greater than that of using MOP strategy with $\lambda_0 = 0.8$ as shown in Fig. 8*b*. Changing the time constant of the LPF strategy may improve SOC_{sc} or power loss. However, the performance is unpredictable and uncontrollable. In contrast, when the proposed MOP algorithm is realised in PV station, the optimisation factor could be preset or updated in real-time, depending on the preference of performance.

6 Conclusion

The HESS is beneficial to suppress the power fluctuation of PV station and to limit the maximum active power change rate at a reasonable range. In this paper, a novel energy management system for battery/SC HESS is proposed. To balance the two major optimisation targets of HESS, i.e. reservation of SOC_{sc} and minimisation of power loss, a linear weighted summation algorithm based on variable weights is proposed to solve an MOP, which could obtain the optimal power sharing ratio between SC and battery.

The simulation and experiment have verified the proposed algorithm, and the results have revealed the advantages of the proposed algorithm: the SOC_{sc} could be reserved to respond to future peak power demand from both directions and high efficiency could be achieved via the consideration of overall energy loss in the MOP, depending on the configuration of the optimisation factor.

7 Acknowledgment

This work was supported by the National Natural Science Foundations of China under Award 51407025.

8 References

1 Eghtedarpour, N., Farjah, E.: 'Distributed charge/discharge control of energy storages in a renewable-energy-based DC micro-grid', *IET Renew. Power Gener.*, 2014, **8**, (1), pp. 45–57
2 Liu, X., Aichhorn, A., Liu, L., *et al.*: 'Coordinated control of distributed energy storage system with tap changer transformers for voltage rise mitigation under high photovoltaic penetration', *IEEE Trans. Smart Grid*, 2012, **3**, (2), pp. 463–472
3 Sugihara, H., Yokoyama, K., Saeki, O., *et al.*: 'Economic and efficient voltage management using customer-owned energy storage systems in a distribution network with high penetration of photovoltaic systems', *IEEE Trans. Power Syst.*, 2013, **28**, (1), pp. 102–111
4 Wang, Y., Lin, X., Pedram, M.: 'Adaptive control for energy storage systems in households with photovoltaic modules', *IEEE Trans. Smart Grid*, 2014, **5**, (2), pp. 992–1001
5 Kim, S., Bae, S., Kang, Y.C., *et al.*: 'Energy management based on the photovoltaic HPCS with an energy storage device', *IEEE Trans. Ind. Electron.*, 2015, **62**, (7), pp. 4608–4617
6 Gee, A.M., Dunn, R.W.: 'Novel battery/supercapacitor hybrid energy storage control strategy for battery life extension in isolated wind energy conversion systems'. Proc. Universities Power Engineering Conf. (UPEC), August/September 2010, pp. 1–6
7 Dougal, R.A., Liu, S., White, R.E.: 'Power and life extension of battery–ultracapacitor hybrids', *IEEE Trans. Compon. Packag. Technol.*, 2002, **25**, (1), pp. 120–131
8 Borhan, H.A., Vahidi, A.: 'Model predictive control of a power-split hybrid electric vehicle with combined battery and ultracapacitor energy storage'. Proc. American Control Conf., June/July 2010, pp. 5031–5036
9 Kawashima, K., Uchida, T., Hori, Y.: 'Development of a novel ultracapacitor electric vehicle and methods to cope with voltage variation'. Proc. IEEE Vehicle Power and Propulsion Conf., September 2009, pp. 724–729
10 Shah, V., Karndhar, S., Maheshwari, R., *et al.*: 'An energy management system for a battery ultracapacitor hybrid electric vehicle'. Proc. Int. Conf. Industrial and Information Systems, December 2009, pp. 408–413
11 Glavin, M., Chan, P., Armstrong, S., *et al.*: 'A stand-alone photovoltaic supercapacitor battery hybrid energy storage system'. Proc. 13th Power Electronics and Motion Control Conf., 2008 (EPE-PEMC 2008), 2008, pp. 1688–1695
12 Zhou, H., Bhattacharya, T., Tran, D., *et al.*: 'Composite energy storage system involving battery and ultracapacitor with dynamic energy management in microgrid applications', *IEEE Trans. Power Electron.*, 2011, **26**, (3), pp. 923–930
13 Barrade, P., Rufer, A.: 'The use of supercapacitors for energy storage in traction systems'. Vehicular Power and Propulsion Symp. (IEEE-VPP 04), Paris, France, October 2004
14 Baisden, A.C., Emadi, A.: 'Advisor-based model of a battery and an ultra-capacitor energy source for hybrid electric vehicles', *IEEE Trans. Veh. Technol.*, 2004, **53**, (1), pp. 199–205
15 Pay, S., Daly, Y.: 'Effectiveness of battery-supercapacitor combination in electric vehicles'. IEEE Proc. Power Tech Conf., June 2003, vol. 3, pp. 1–6
16 Allgre, A., Trigui, R., Bouscayrol, A.: 'Different energy management strategies of hybrid energy storage system (HESS) using batteries and supercapacitors for vehicular applications'. Proc. IEEE Vehicle and Power Propulsion Conf., September 2010, pp. 1–6
17 Wong, J., Idris, N., Anwari, M., *et al.*: 'A parallel energy-sharing control for fuel cell-battery-ultracapacitor hybrid vehicle'. Proc. IEEE Energy Conversion Congress and Exposition, September 2011, pp. 2923–2929
18 Garcia, F., Ferreira, A., Pomilio, J.: 'Control strategy for battery ultracapacitor hybrid energy storage system'. Proc. 24th Annual IEEE Applied Power Electronics Conf. and Exposition, February 2009, pp. 826–832
19 Liu, F., Liu, J., Zhou, L.: 'A novel control strategy for hybrid energy storage system to relieve battery stress'. 2010 Second IEEE Int. Symp. on Power Electronics for Distributed Generation Systems, 2010

20 Laldin, O., Moshirvaziri, M., Trescases, O.: 'Predictive algorithm for optimizing power flow in hybrid ultracapacitor/battery storage systems for light electric vehicles', *IEEE Trans. Power Electron.*, 2013, **28**, (8), pp. 3882–3895
21 Choi, M.-E., Kim, S.-W., Seo, S.-W.: 'Energy management optimization in a battery/supercapacitor hybrid energy storage system', *IEEE Trans. Smart Grid*, 2012, **3**, (1), pp. 463–472
22 Romaus, C., Bocker, J., Witting, K., *et al.*: 'Optimal energy management for a hybrid energy storage system combining batteries and double layer capacitors'. Proc. IEEE Energy Conversion Congress and Exposition, September 2009, pp. 1640–1647
23 China State Grid: 'The technology regulations of grid-connected photovoltaic power station', 2011
24 Jiang, W., Kai, L., Hu, R.: 'Novel modeling and design of a dual half bridge DC–DC converter applied in supercapacitor energy storage system', *Electr. Power Compon. Syst.*, 2014, **42**, (13), pp. 1398–1408
25 Sherkat, V.R., Ikura, Y.: 'Experience with interior point optimization software for a fuel planning application', *IEEE Trans. Power Syst.*, 1994, **9**, (2), pp. 833–840
26 Tran, D., Zhou, H., Khambadkone, A.M.: 'Energy management and dynamic control in composite energy storage system for micro-grid applications'. Proc. IECON 2010 – 36th Annual Conf. on IEEE Industrial Electronics Society, November 2010, pp. 1818–1824